Nuclear Materials and Energy 33 (2022) 101250

Contents lists available at ScienceDirect

Nuclear Materials and Energy

journal homepage: www.elsevier.com/locate/nme

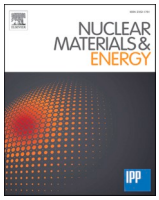

Control of tungsten impurity source and edge transport using different gas injection with full tungsten divertor on EAST

R. Ding [a,*], G.L. Xu [a,*], H. Wang [a], F. Ding [a], L. Zhang [a], Q. Zhang [a], K.D. Li [a], J.B. Liu [a], S. Brezinsek [b], A. Kirschner [b], S.X. Wang [a], B.F. Gao [a], L.Y. Meng [a], L. Wang [a], H. Xie [a], H. Si [a], R. Yan [a], D.H. Zhu [a], J.L. Chen [a]

[a] Institute of Plasma Physics, Chinese Academy of Sciences, Hefei, China
[b] Forschungszentrum Jülich GmbH, Institut für Energie- und Klimaforschung, Jülich, Germany

A B S T R A C T

Tungsten (W) erosion and edge transport are investigated for EAST L-mode discharges with different gas injection. It is found that W erosion can be suppressed or mitigated by Ne or D_2 seeding when divertor detachment is achieved. Compared to edge D_2 fueling, Ne seeding from the divertor target is favorable for full detachment condition and thus W erosion suppression. Increasing the upstream plasma density by edge D_2 fueling can affect the divertor condition, which may lead to a W erosion mitigation. D_2 puffing at divertor target is less effective on increasing the upstream plasma density than OMP D_2 puffing, and thus it is less effective on reduction of W erosion rates. W gross erosion profiles with different amount of injected D_2 at the divertor are reproduced by a mixed material W erosion model, which indicates that there exist a Li-C overlayer on the W surface of EAST divertor. Ne and D_2 injection are also found to have different impact on the normalized core W density. For the attached divertor condition, divertor Ne seeding will increase W leakage, but a suitable D_2 fueling from divertor target can strengthen the edge W screening. After the divertor detachment, although the W source is dramatically reduced, the W core density is kept in a high level for the Ne seeding discharges, and even increased for the D_2 fueling discharges.

Introduction

Tungsten (W) impurity contamination is a key issue for long-pulse high-performance plasma operation in tokamaks with W plasma-facing materials. To reduce the W impurity level in the core plasma, it is important to understand the physics processes of W impurity source and edge transport. It has long been verified by multiple tokamaks that the effective sputtering yields of tungsten at the divertor have a strong correlation with the target electron temperature [1–3]. Gas puffing from the edge plasma is an effective way to manipulate the target electron temperature and heat flux density [4–8]. Previous experiments on DIII-D show that local gas puffing can suppress W erosion significantly [9,10]. Meanwhile, seeding impurities also has to be used as radiators for heat exhaust of ITER and future fusion tokamaks with W divertor [11–13], but they may induce additional W sputtering source due to higher sputtering yields by impurities. Therefore, it is important to study the effects of different gas injection conditions on W source and edge transport in current devices.

Previous experimental results based on EAST upper W divertor reveal that the divertor W erosion rate is closely related to both the heating power and the upstream plasma density [14,15]. Due to the routinely lithium coating for wall conditioning in EAST, W impurity source is also determined by the wall condition. Real-time wall conditioning including lithium and boron powder injection is also found to be an effective way to suppress divertor W erosion [16,17]. Simulation results from both ERO and SOLPS indicate that the W erosion of EAST divertor strongly depends on the impurity fraction in background plasma, such as the intrinsic impurity of carbon [18–20].

The EAST lower divertor has been upgraded from a graphite divertor to a W divertor with both horizontal and vertical targets since 2021 [21,22]. The new actively water-cooled divertor has a strong power handling ability, and it provides a good platform to study W impurity source and edge transport in an ITER-like closed divertor geometry. Previous edge impurity seeding experiments on EAST reveal that Ne seeding has a better compatibility with the core plasma performance than Ar due to the relatively lower radiation losses in the core region [23,24]. In this paper, W erosion and edge transport under different edge Ne and D_2 gas puffing conditions with the outer strike point (OSP) fixed on the corner of EAST lower outer W divertor are studied. A brief description of the experiments is given in section 2, followed by a discussion of the experimental results in section 3 and conclusions in section 4.

* Corresponding authors.
E-mail addresses: rding@ipp.ac.cn (R. Ding), guoliang.xu@ipp.ac.cn (G.L. Xu).

https://doi.org/10.1016/j.nme.2022.101250
Received 1 July 2022; Received in revised form 21 August 2022; Accepted 8 September 2022
Available online 14 September 2022

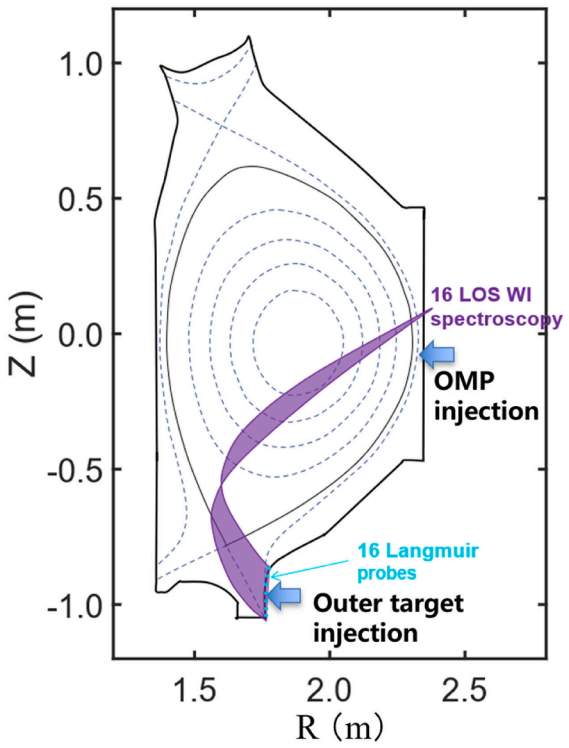

Fig. 1. The EAST fist wall and magnetic equilibrium configuration of discharge 103,243 at 5.07 s. The 400.9 nm WI spectroscopy and Langmuir probes covering the lower outer divertor target are also illustrated. Ne and D_2 gases can be injected from either the outer divertor region or OMP.

Experimental setup

EAST is a D-shaped fully superconducting tokamak with a molybdenum first wall and tungsten upper and lower divertors. The experiments shown in this manuscript were carried out based on a series of EAST lower single-null L-mode discharges with the outer strike point at the corner of the outer lower W divertor, as shown in Fig. 1. Ne gas was seeded into the edge plasma and compared with the D_2 gas puffing discharges. The gas injection location is at the outer divertor target near the strike point or from the outer mid-plane (OMP), as illustrate in Fig. 1. Electron cyclotron resonance heating (ECRH) [25] and lower hybrid wave (LHW) heating [26] were used with a total heating power about 3.5 MW for these discharges.

The distribution of W source along the lower outer divertor target was characterized by a multichannel visible spectroscopy system observing WI line emission at 400.9 nm [14]. The local plasma parameters including the electron temperature (T_e) and the ion saturation current (J_{sat}) on the divertor target were measured directly by Langmuir probe arrays [27], which contains 16 triple Langmuir probes located on both the vertical and horizontal targets of the lower outer divertor. W impurity density in the core plasma can be obtained by the tungsten unresolved transition array (WUTA) [28], with the core plasma density and temperature distribution measured by the polarimeter-interferometer system (POINT) [29] and the electron cyclotron emission (ECE) [30] respectively.

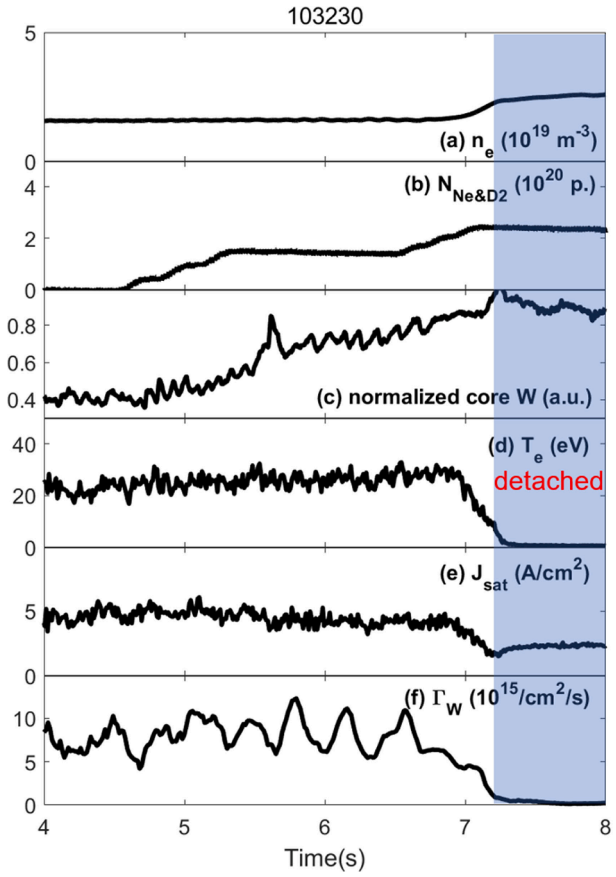

Fig. 2. Time evolution of the key parameters for discharge #103230 with 1:1 Ne&D_2 injected from the divertor target. (a) Line-averaged electron density, (b) total gas puffing amount, (c) the normalized core W density, (d) electron temperature near the OSP with r-r_{sep} = 1.87 cm, (e) ion saturation current near the OSP with r-r_{sep} = 1.87 cm, and (f) W gross erosion rate near the OSP with r-r_{sep} = 1.84 cm.

Experimental results and discussion

Gas injection from the divertor target

Due to the strong impact on the core plasma performance by pure Ne seeding on EAST [31], a mixed Ne and D_2 injection method is applied with the ratio of Ne atoms to D_2 molecules of 1:1. As shown in Fig. 2, for discharge #103230, Ne&D_2 mixed gas is injected from the outer divertor target from 4.5 s to 7 s. The auxiliary heating power includes P_{EC} = 1.4 *MW* and P_{LH} = 2.0 *MW*, and the plasma current is 500 kA. The line-averaged electron density and the total gas puffing amount are plotted in Fig. 2(a) and 2(b), with the core W density normalized by maximum value plotted in Fig. 2(c). T_e and J_{sat} measured by the Langmuir probe near the OSP are shown in Fig. 2(d) and 2(e), with the strongest W erosion rate near the OSP derived from the 400.9 nm WI spectroscopy plotted in Fig. 2(f). All these parameters are plotted for the current flattop phase of the discharge from 4 s to 8 s.

With the increase of total injected amount of Ne&D_2, a fully detached divertor condition is finally achieved and then W erosion is well suppressed after achieving the divertor detachment. But before detachment, W erosion rate does not change much although the particle flux density impinging to the divertor target slightly decreases. Meanwhile, the

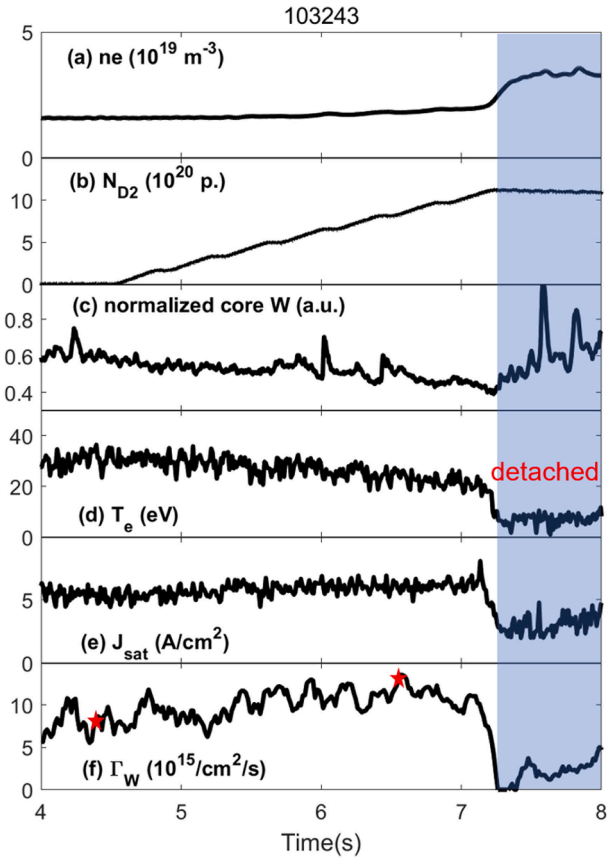

Fig. 3. Time evolution of the key parameters for discharge #103243 with pure D_2 injected from the divertor target. (a) Line-averaged electron density, (b) total gas puffing amount, (c) the normalized core W density, (d) electron temperature near the OSP with r-r_{sep} = 1.87 cm, (e) ion saturation current near the OSP with r-r_{sep} = 1.87 cm, and (f) W gross erosion rate near the OSP with r-r_{sep} = 1.84 cm. The two time slices before and after D_2 puffing (t = 4.4 s and t = 6.6 s, marked by red stars) are selected for W erosion modeling. (For interpretation of the references to colour in this figure legend, the reader is referred to the web version of this article.)

normalized core W density increases significantly with the increase of Ne&D_2 seeding amount, which means a weaker W edge screening.

Pure D_2 is also injected from the divertor target to investigate the influence on W erosion and transport, as shown in Fig. 3. The main parameters including auxiliary heating power and plasma current of discharge #103243 is the same as #103230. D_2 is injected from 4.5 s to 7.2 s until divertor detachment is achieved. Similar to the Ne seeding discharge, W erosion rate is significantly reduced with divertor D_2 fueling only after the onset of detachment. However, relatively higher gas puffing amount and upstream plasma density are needed for pure D_2 fueling to achieve the divertor detachment than that of the Ne&D_2 seeding, which demonstrates the different power dissipation ability between D_2 and Ne.

Before divertor detachment, a slight increase of W erosion rate is observed with divertor D_2 fueling. A newly developed Li-C-W mixed material model [32] is applied to calculate the W erosion profile along the lower outer divertor target for different time slices before and after D_2 fueling. The selected time slices are marked by red stars in Fig. 3, which are t = 4.4 s and t = 6.6 s respectively. As shown in Fig. 4, by taking the target plasma parameters (T_e and J_{sat} from Langmuir probes and fitted by Eich function [33]), the W erosion profiles for both t = 4.4 s and t = 6.6 s are well reproduced. Note that a 10 Å Li-C overlayer on the W surface are assumed in the mixed-material W erosion model, due to the reason that Li and C are the most two important intrinsic impurities in EAST plasma and can be deposited on the W surface [32,34–36]. Modeling results demonstrate that the slight increase of W erosion rate before detachment is mainly due to the increase of the impinging particle flux density caused by D_2 fueling.

Gas injection from the OMP

OMP D_2 injection is also an effective way to increase the upstream plasma density and thus manipulate the divertor target conditions, as plotted in Fig. 5. The auxiliary heating power of discharge 103,246 are $P_{EC} = 1.25\ MW$ and $P_{LH} = 2.5\ MW$, and the plasma current is 500 kA. OMP D_2 fueling starts from 4 s to 7 s, as shown in Fig. 5(b). The impact on upstream plasma density is obviously faster than that of the divertor gas injection cases aforementioned. Unlike D_2 puffing from the divertor target, a decrease of W gross erosion rate is observed before the onset of detachment for the OMP D_2 puffing discharge. W erosion mitigation is mainly caused by the reduction of T_e on the divertor target, which has a strong correlation with the upstream plasma density according to the two-point edge plasma model [4]. Divertor detachment is achieved at around 5.5 s, and W erosion at the divertor target is strongly mitigated after the detachment.

However, the degree of divertor detachment achieved by D_2 puffing cases are not as deep as the Ne gas puffing case, as shown in Fig. 6. Owing to the strong power dissipation ability of Ne, a fully detachment is sustained with a mixed Ne&D_2 seeding, which suppresses W erosion on the whole divertor target completely. Whereas for the D_2 injection discharges, only partial detachment is achieved. Therefore, compared to D_2 injection, Ne seeding from the divertor target is more favorable for a fully divertor detachment and thus W erosion suppression.

W impurity screening and core contamination

Ne and D_2 injection also show different impact on the edge W screening effects. Fig. 7 is the comparison of the normalized core W density for Ne and D_2 puffing discharges. For the Ne seeding discharge, an increase of the core W density is observed with a stable W source before the onset of divertor detachment, which means a degradation of edge W screening as mentioned before. However, the core W density for D_2 puffing discharges decreases before the onset of detachment. For the divertor D_2 puffing discharge, the W source slightly increases before detachment (as shown in Fig. 3), so W screening is reinforced consequently. While for the OMP D_2 puffing discharge, W source is decreased consistent with the core W density before detachment as shown in Fig. 5, and therefore, the impact on W screening is not obvious.

After the onset of detachment, although W source is suppressed for all these three discharges, the W core density is kept at a high level for the Ne seeding discharge and even strongly increased for the D_2 puffing discharges. The enhancement of core W density is due to the improvement of particle confinement in the core plasma after the onset of detachment. Fig. 8 shows electron density profiles in the core plasma measured by POINT for time slices before and after divertor detachment of discharges #103230, #103243 and #103246. An increase of core plasma density and its gradient after the onset of detachment is observed which also indicates an improvement of particle confinement in the core

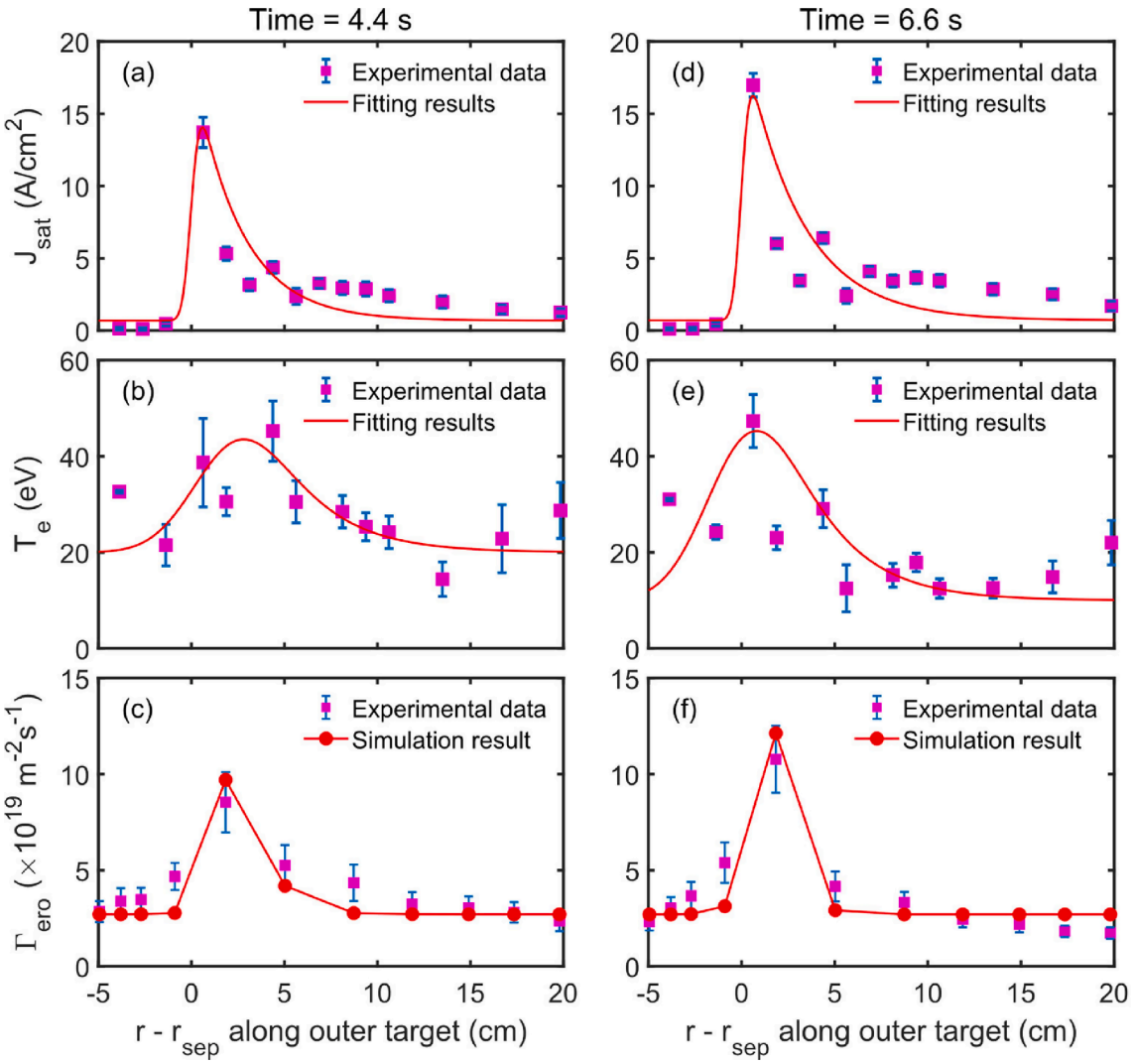

Fig. 4. Divertor target profiles of ion saturation current, electron temperature and W erosion rate for $t = 4.4$ s (figure (a)-(c)) and $t = 6.6$ s (figure (d)-(f)) of discharge 103243. Markers are experimental data, and red lines are fitting results in figure (a)、(b)、(d)、(e) and modeling results in figure (c)、(f). (For interpretation of the references to colour in this figure legend, the reader is referred to the web version of this article.)

plasma. Studies of W distribution and transport in the core plasma during divertor detachment needs to be done in the future.

Conclusions

With the newly installed EAST lower W divertor, W source and edge transport are experimentally investigated for different Ne&D_2 gas injection conditions. Experimental results reveal that W erosion on the whole divertor target can be well suppressed or mitigated by suitable edge Ne or D_2 injection when divertor detachment is achieved. Compared to D_2 puffing, Ne seeding from the divertor region is favorable for fully detachment condition and thus W erosion suppression. D_2 injection from both divertor target and OMP can also induce a partial detachment condition by strongly increase the upstream plasma density, and therefore mitigate the divertor W erosion.

Ne and D_2 injection show different impact on the edge W screening and core W contamination. For the Ne seeding discharge, edge W screening becomes weaker, and a core W accumulation is observed accordingly with Ne seeding. However, for discharges of D_2 injection from both divertor target and OMP, a decrease of W core density is observed before divertor detachment. A W screening enhancement is obtained during the attached divertor condition due to D_2 injection. After the divertor detachment, W core density is strongly increased for D_2 injection discharges and still kept in a high level for the Ne injection discharge, in spite of that the W source from the divertor is well suppressed. Although impurity seeding is an effective way to reduce divertor heat loads, it may cause degradation of edge W screening, and this may lead to the core W accumulation which can dramatically affect the core plasma performance. The physics of edge W screening degradation observed in the EAST experiments remains to be understood by dedicated experiments and modeling in the future.

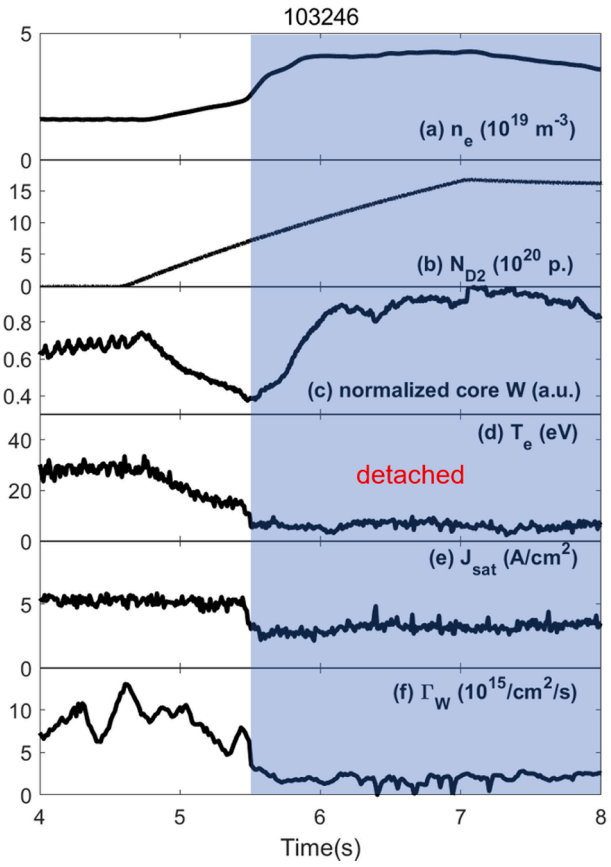

Fig. 5. Time evolution of the key parameters for discharge #103246 with pure D_2 injected from OMP. (a) Line-averaged electron density, (b) total gas puffing amount, (c) the normalized core W density, (d) electron temperature near the OSP with r-r_{sep} = 1.87 cm, (e) ion saturation current near the OSP with r-r_{sep} = 1.87 cm, and (f) W gross erosion rate near the OSP with r-r_{sep} = 1.84 cm.

CRediT authorship contribution statement

R. Ding: Methodology, Conceptualization, Investigation, Validation, Formal analysis, Writing – original draft, Writing – review & editing, Resources, Supervision, Project administration, Funding acquisition. **G. L. Xu:** Investigation, Validation, Formal analysis, Visualization, Writing – review & editing. **H. Wang:** Investigation, Validation, Formal analysis. **F. Ding:** Investigation, Validation. **L. Zhang:** Investigation, Validation. **Q. Zhang:** Investigation, Validation. **K.D. Li:** Investigation, Validation. **J.B. Liu:** Investigation, Validation. **S. Brezinsek:** Validation. **A. Kirschner:** Validation. **S.X. Wang:** Investigation, Validation. **B.F. Gao:** Investigation, Validation. **L.Y. Meng:** Investigation, Validation. **L. Wang:** Investigation, Validation. **H. Xie:** Validation. **H. Si:** Validation. **R. Yan:** Validation, Funding acquisition. **D.H. Zhu:** Validation, Funding acquisition. **J.L. Chen:** Supervision, Funding acquisition.

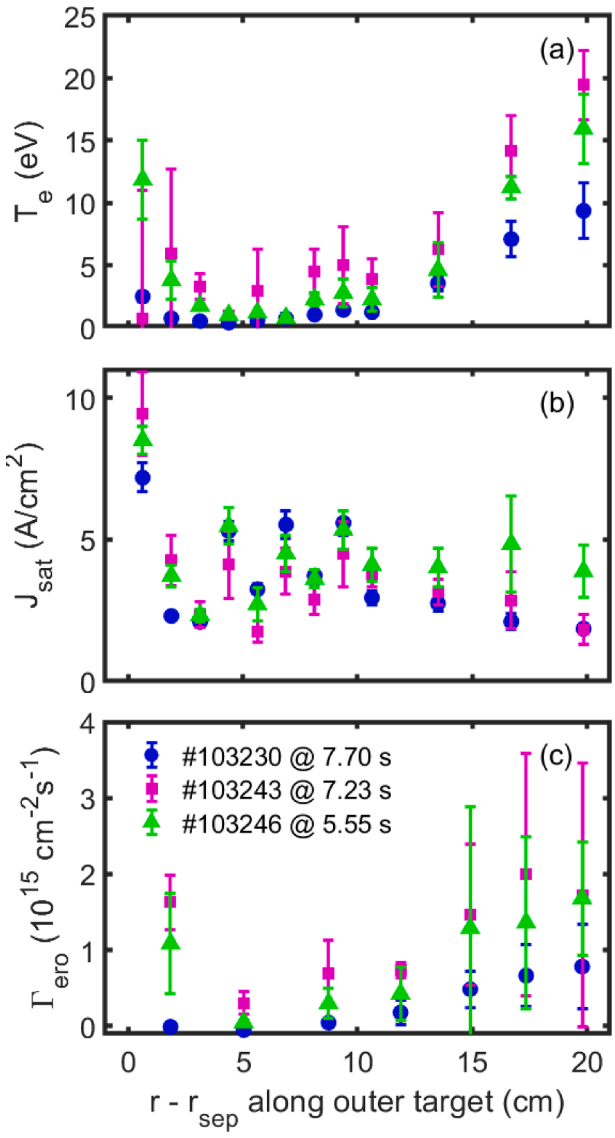

Fig. 6. The (a) electron temperature, (b) ion saturation current, and (c) corresponding W erosion profiles along the outer divertor target for the detached divertor condition in #103230 (blue dots), # 103,243 (pink dots), and #103246 (green dots). (For interpretation of the references to colour in this figure legend, the reader is referred to the web version of this article.)

Declaration of Competing Interest

The authors declare that they have no known competing financial interests or personal relationships that could have appeared to influence the work reported in this paper.

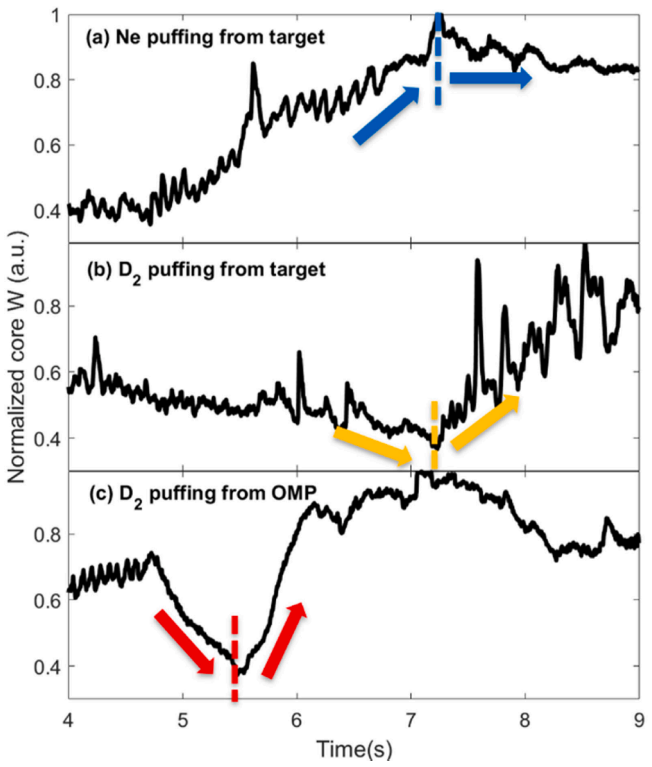

Fig. 7. The time evolution of the normalized core W density for discharges of (a) #103230, (b) #103243 and (c) #103246. Dashed lines refer to the onset of divertor detachment.

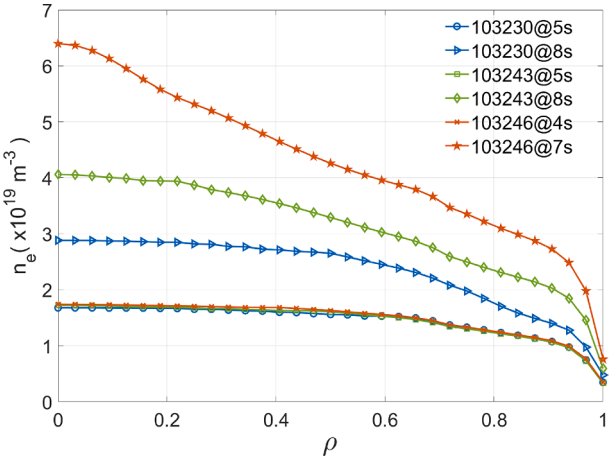

Fig. 8. Electron density profiles in the core plasma measured by POINT for time slices before and after divertor detachment of discharges #103230, #103243 and #103246.

Acknowledgement

The work was supported by the National Natural Science Foundation of China under Contract Nos. 12022511 and 12005143, National Key Research and Development Program of China under contract No. the National MCF Energy R&D Program of China under contract No. 2022YFE03180100 and 2019YFE03080100, the Key Research Program of Frontier Sciences, CAS with Grant No. ZDBS-LY-SLH010, the Science Foundation of Institute of Plasma Physics, Chinese Academy of Sciences (No. DSJJ-2021-02).

References

[1] H. Mao, F. Ding, G.-N. Luo, Z. Hu, X. Chen, F. Xu, J. Hu, G. Zuo, Z. Sun, Y. Yu, J. Wu, L. Wang, Y. Duan, J. Xu, J. Chen, Z. Yang, R. Ding, H. Xie, The impacts of lithium and silicon coating on the W source in EAST, Nucl. Mater. Energy 12 (2017) 447–452.
[2] R. Dux, V. Bobkov, A. Herrmann, A. Janzer, A. Kallenbach, R. Neu, M. Mayer, H. W. Müller, R. Pugno, T. Pütterich, V. Rohde, A.C.C. Sips, Plasma-wall interaction and plasma behaviour in the non-boronised all tungsten ASDEX Upgrade, J. Nucl. Mater. 390–391 (2009) 858–863, https://doi.org/10.1016/j.jnucmat.2009.01.225.
[3] G.J. Van Rooij, J.W. Coenen, L. Aho-Mantila, S. Brezinsek, M. Clever, R. Dux, M. Groth, K. Krieger, S. Marsen, G.F. Matthews, A. Meigs, R. Neu, S. Potzel, T. Pütterich, J. Rapp, M.F. Stamp, Tungsten divertor erosion in all metal devices: Lessons from the ITER like wall of JET, J. Nucl. Mater. 438 (2013) S42–S47, https://doi.org/10.1016/j.jnucmat.2013.01.007.
[4] P.C. Stangeby, The plasma boundary of magnetic fusion devices, CRC Press, 2000.
[5] M.A. Mahdavi, S.L. Allen, D.R. Baker, B. Bastasz, N.H. Brooks, D. Buchenauer, R. B. Campbell, J.W. Cuthbertson, T.E. Evans, M.E. Fenstermacher, D.F. Finkenthal, J. Foote, D.N. Hill, D.L. Hillis, F.L. Hinton, J. Hogan, A.W. Howald, A.W. Hyatt, G. L. Jackson, R. Jong, S. Konoshima, C. Lasnier, A.W. Leonard, S.I. Lippmann, R. Maingi, M.M. Menon, P.K. Mioduszewski, R.A. Moyer, H. Ogawa, T.W. Petrie, G. D. Porter, M.E. Rensink, T.D. Rognlein, M.J. Schaffer, K.M. Schaubel, D.L. Sevier, J. P. Smith, G.M. Staebler, G.T. Sager, R.D. Stambaugh, D. Thomas, M.R. Wade, J. G. Watkins, F. Weschenfelder, W.P. West, D.G. Whyte, J. Winter, C.P.C. Wong, R. D. Wood, Divertor heat and particle control experiments on the DIII-D tokamak, J. Nucl. Mater. 220-222 (1995) 13–24.
[6] D.N. Hill, S.L. Allen, N.H. Brooks, Divertor research on the DIII-D tokamak, 1994.
[7] M. Bakhtiari, H. Tamai, Y. Kawano, G.J. Kramer, A. Isayama, T. Nakano, Y. Kamiya, R. Yoshino, Y. Miura, Y. Kusama, Study of plasma termination using high-Z noble gas puffing in the JT-60U tokamak, Nucl. Fusion. 45 (2005) 318.
[8] G.F. Matthews, Plasma detachment from divertor targets and limiters, J. Nucl. Mater. 220-222 (1995) 104–116.
[9] R. Ding, D.L. Rudakov, P.C. Stangeby, W.R. Wampler, T. Abrams, S. Brezinsek, A. Briesemeister, I. Bykov, V.S. Chan, C.P. Chrobak, J.D. Elder, H.Y. Guo, J. Guterl, A. Kirschner, C.J. Lasnier, A.W. Leonard, M.A. Makowski, A.G. McLean, P. B. Snyder, D.M. Thomas, D. Tskhakaya, E.A. Unterberg, H.Q. Wang, J.G. Watkins, High-Z material erosion and its control in DIII-D carbon divertor, Nucl. Mater. Energy. 12 (2017) 247–252.
[10] R. Ding, D.L. Rudakov, P.C. Stangeby, W.R. Wampler, T. Abrams, S. Brezinsek, A. Briesemeister, I. Bykov, V.S. Chan, C.P. Chrobak, Advances in understanding of high-Z material erosion and re-deposition in low-Z wall environment in DIII-D, Nucl. Fusion. 57 (2017) 56016.
[11] X.J. Liu, G.L. Xu, R. Ding, G.Z. Jia, C.F. Sang, H. Si, F.F. Nian, Z.S. Yang, G.Q. Li, V. S. Chan, Simulation studies of divertor power exhaust with neon seeding for CFETR with GW-level fusion power, Phys. Plasmas. 27 (2020) 92508.
[12] A. Kallenbach, M. Bernert, R. Dux, L. Casali, T. Eich, L. Giannone, A. Herrmann, R. McDermott, A. Mlynek, H.W. Müller, F. Reimold, J. Schweinzer, M. Sertoli, G. Tardini, W. Treutterer, E. Viezzer, R. Wenninger, M. Wischmeier, Impurity seeding for tokamak power exhaust: from present devices via ITER to DEMO, Plasma Phys. Control. Fusion. 55 (12) (2013) 124041, https://doi.org/10.1088/0741-3335/55/12/124041.
[13] H.D. Pacher, A.S. Kukushkin, G.W. Pacher, V. Kotov, R.A. Pitts, D. Reiter, Impurity seeding in ITER DT plasmas in a carbon-free environment, J. Nucl. Mater. 463 (2015) 591–595.
[14] H. Mao, F. Ding, G.-N. Luo, Z. Hu, X. Chen, F. Xu, Z. Yang, J. Chen, L. Wang, R. Ding, A multichannel visible spectroscopy system for the ITER-like W divertor on EAST, Rev. Sci. Instrum. 88 (2017) 43502.
[15] F. Ding, G.-N. Luo, X. Chen, H. Xie, R. Ding, C. Sang, H. Mao, Z. Hu, J. Wu, Z. Sun, L. Wang, Y. Sun, J. Hu, Plasma–tungsten interactions in experimental advanced superconducting tokamak (EAST), Tungsten 1 (2) (2019) 122–131.
[16] W. Xu, J.S. Hu, Z. Sun, R. Maingi, G.Z. Zuo, Y.Z. Qian, C.L. Li, L. Zhang, X.C. Meng, M. Huang, Comparison of active impurity control between lithium and boron powder real-time injection in EAST, Phys. Scr. 96 (2021), 124034.
[17] W. Xu, J.S. Hu, R. Maingi, Z. Sun, G.Z. Zuo, D.K. Mansfield, A. Diallo, K. Tritz, M. Huang, X.C. Meng, L. Wang, Y.Z. Qian, L. Zhang, F. Ding, R. Lunsford, T. Osborne, J.G. Li, Real-time reduction of tungsten impurity influx using lithium powder injection in EAST, Fusion Eng. Des. 137 (2018) 202–208.
[18] H. Xie, R. Ding, A. Kirschner, J.L. Chen, F. Ding, H.M. Mao, W. Feng, D. Borodin, L. Wang, ERO modelling of tungsten erosion and re-deposition in EAST L mode discharges, Phys. Plasmas. 24 (2017) 92512.
[19] Q. Zhou, C. Sang, G. Xu, R. Ding, X. Zhao, Y. Wang, D. Wang, The transport of tungsten impurities induced by the intrinsic carbon during upper-single null discharge on EAST tokamak, Nucl. Mater. Energy 25 (2020), 100849.
[20] C. Sang, R. Ding, X. Bonnin, L. Wang, D. Wang, E. Team, Effects of carbon impurities on the power radiation and tungsten target erosion in EAST, Phys. Plasmas 25 (2018) 72511.
[21] G.S. Xu, L. Wang, D.M. Yao, G.Z. Jia, C.F. Sang, X.J. Liu, Y.P. Chen, H. Si, Z.S. Yang, H.Y. Guo, Physics design of new lower tungsten divertor for long-pulse high-power operations in EAST, Nucl. Fusion 61 (2021), 126070.
[22] C. Sang, Q. Zhou, G. Xu, L. Wang, Y. Wang, X. Zhao, C. Zhang, R. Ding, G. Jia, D. Yao, Design of EAST lower divertor by considering target erosion and tungsten ion transport during the external impurity seeding, Nucl. Fusion 61 (2021) 66004.
[23] K. Li, Z. Yang, H. Wang, G. Xu, Q. Yuan, H. Guo, D. Eldon, A. Hyatt, D. Humphreys, M. Chen, Comparison of divertor behavior and plasma confinement between argon and neon seeding in EAST, Nucl. Fusion 61 (2021) 66013.

[24] D. Eldon, H.Q. Wang, L. Wang, J. Barr, S. Ding, A. Garofalo, X.Z. Gong, H.Y. Guo, A.E. Järvinen, K.D. Li, An analysis of controlled detachment by seeding various impurity species in high performance scenarios on DIII-D and EAST, Nucl. Mater. Energy 27 (2021), 100963.
[25] H. Xu, X. Wang, F. Liu, J. Zhang, Y. Huang, J. Shan, D. Wu, H. Hu, B. Li, M. Li, Development and preliminary commissioning results of a long pulse 140 GHz ECRH system on EAST tokamak, Plasma Sci. Technol. 18 (2016) 442.
[26] J. Li, B. Wan, Recent progress in RF heating and long-pulse experiments on EAST, Nucl. Fusion 51 (2011) 94007.
[27] J.C. Xu, L. Wang, G.S. Xu, W. Feng, H. Liu, J.B. Liu, W. Zhang, T.F. Ming, C.-S. Yip, G.Z. Deng, S.Y. Dai, D.M. Yao, G.N. Luo, H.Y. Guo, Upgrade design of lower divertor Langmuir probe diagnostic system in the EAST Tokamak, IEEE Trans. Plasma Sci. 46 (5) (2018) 1331–1337.
[28] L. Zhang, S. Morita, Z. Wu, Z. Xu, X. Yang, Y. Cheng, Q. Zang, H. Liu, Y. Liu, H. Zhang, T. Ohishi, Y. Chen, L. Xu, C. Wu, Y. Duan, W. Gao, J. Huang, X. Gong, L. Hu, A space-resolved extreme ultraviolet spectrometer for radial profile measurement of tungsten ions in the Experimental Advanced Superconducting Tokamak, Nucl. Instrum. Methods Phys. Res. Sect. A Accel. Spectrometers, Detect. Assoc. Equip. 916 (2019) 169–178.
[29] H.Q. Liu, Y.X. Jie, W.X. Ding, D.L. Brower, Z.Y. Zou, W.M. Li, Z.X. Wang, J.P. Qian, Y. Yang, L. Zeng, Faraday-effect polarimeter-interferometer system for current density measurement on EAST, Rev. Sci. Instrum. 85 (2014) 11D405.
[30] Y. Liu, H. Zhao, T. Zhou, X. Liu, Z. Zhu, X. Han, S. Schmuck, J. Fessey, P. Trimble, C.W. Domier, N.C. Luhmann, A. Ti, E. Li, B. Ling, L. Hu, X.i. Feng, A. Liu, W. L. Rowan, H. Huang, P.E. Phillips, Overview of the electron cyclotron emission measurements on EAST, Fusion Eng. Des. 136 (2018) 72–75.
[31] L. Wang, H.Y. Guo, F. Ding, Y.W. Yu, Q.P. Yuan, G.S. Xu, H.Q. Wang, L. Zhang, R. Ding, J.C. Xu, Advances in plasma–wall interaction control for H-mode operation over 100 s with ITER-like tungsten divertor on EAST, Nucl. Fusion 59 (2019) 86036.
[32] G. Xu, R. Ding, F. Ding, X. Chen, X. Qian, S. Brezinsek, X. Gao, Q. Zang, L. Wang, Y. Jie, P. Yan, J. Chen, J. Li, Y. Wan, An interpretive model for the double peaks of divertor tungsten erosion during type-I ELMs in EAST, Nucl. Fusion 61 (8) (2021) 086011, https://doi.org/10.1088/1741-4326/ac086a.
[33] A.U. Team, T. Eich, B. Sieglin, A. Scarabosio, W. Fundamenski, R.J. Goldston, A. Herrmann, Inter-ELM power decay length for JET and ASDEX Upgrade: measurement and comparison with heuristic drift-based model, Phys. Rev. Lett. 107 (2011) 215001.
[34] C. Li, D. Zhao, Z. Hu, X. Wu, G.-N. Luo, J. Hu, H. Ding, Characterization of deuterium retention and co-deposition of fuel with lithium on the divertor tile of EAST using laser induced breakdown spectroscopy, J. Nucl. Mater. 463 (2015) 915–918.
[35] C. Li, Y. Wang, X. Wu, H. Li, J. Hu, J. Chen, G.-N. Luo, H. Ding, Compositions and chemical states on the co-deposition layer of lithiated tungsten of plasma-facing components of EAST, Nucl. Mater. Energy. 12 (2017) 1209–1213.
[36] R. Yan, J. Peng, R. Ding, Y. Li, X. Yin, B. Wang, J. Chen, Surface recovery of the CXRS first mirror of EAST, IEEE Trans. Plasma Sci. 47 (4) (2019) 1769–1773.